Cell Reports

Report

MEK Inhibitors Reverse Growth of Embryonal Brain Tumors Derived from Oligoneural Precursor Cells

Graphical Abstract

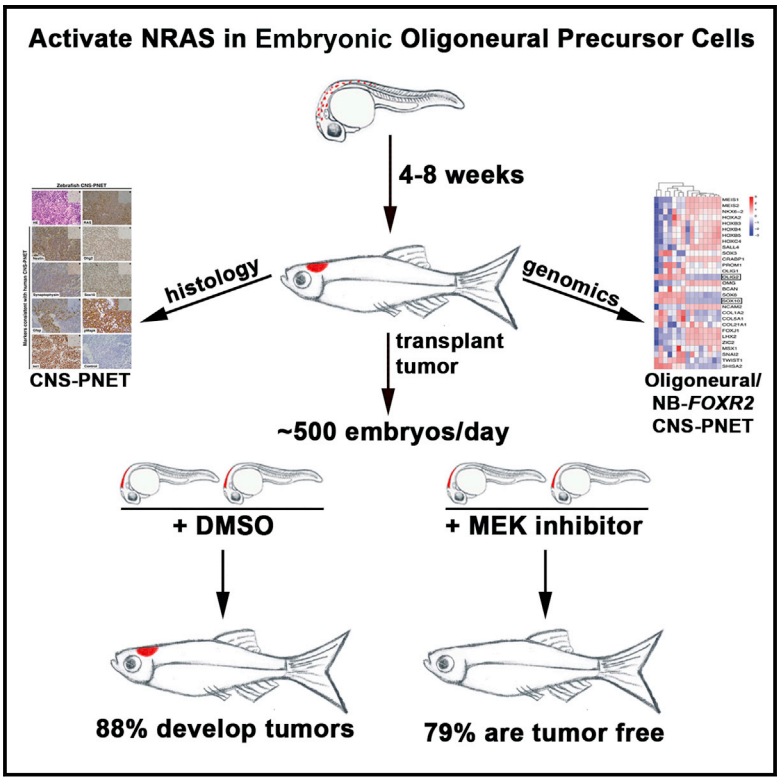

Authors

Katarzyna Modzelewska, Elena F. Boer, Timothy L. Mosbruger, ..., Cicely A. Jette, Annie Huang, Rodney A. Stewart

Correspondence

rodney.stewart@hci.utah.edu

In Brief

Modzelewska et al. generate a zebrafish model of CNS-PNET driven by NRAS activation in *Olig2*$^{+}$/*Sox10*$^{+}$ oligoneural precursor cells. Molecular and genomic analyses show that the zebrafish brain tumors closely resemble the oligoneural/NB-*FOXR2* CNS-PNET subgroup. Finally, an embryonic brain tumor transplantation assay designed to screen drugs shows that MEK inhibitors can eradicate these tumors in vivo.

Highlights

- Subsets of CNS-PNETs express oligodendrocyte precursor cell genes *SOX10* and *OLIG2*
- Activating NRAS/MAPK signaling in OPCs generates CNS-PNET-like tumors in zebrafish
- Cancer genomes of zebrafish and human NB-*FOXR2* CNS-PNETs are highly conserved
- MEK inhibitors are identified as a potential treatment for oligoneural/NB-*FOXR2* CNS-PNETs

Accession Numbers

GSE80768

Modzelewska et al., 2016, Cell Reports *17*, 1255–1264
October 25, 2016
http://dx.doi.org/10.1016/j.celrep.2016.09.081

CellPress

Cell Reports
Report

MEK Inhibitors Reverse Growth of Embryonal Brain Tumors Derived from Oligoneural Precursor Cells

Katarzyna Modzelewska,[1] Elena F. Boer,[1] Timothy L. Mosbruger,[1] Daniel Picard,[6] Daniela Anderson,[1] Rodney R. Miles,[2] Mitchell Kroll,[1] William Oslund,[1] Theodore J. Pysher,[3,4] Joshua D. Schiffman,[1,5] Randy Jensen,[1] Cicely A. Jette,[1] Annie Huang,[6] and Rodney A. Stewart[1,7,*]

[1]Department of Oncological Sciences and Huntsman Cancer Institute, University of Utah School of Medicine, Salt Lake City, UT 84112, USA
[2]Department of Pathology and ARUP Laboratories, University of Utah, 500 Chipeta Way, Salt Lake City, UT 84108, USA
[3]Department of Pathology, University of Utah School of Medicine, Salt Lake City, UT 84112, USA
[4]Primary Children's Hospital/Intermountain Healthcare, Salt Lake City, UT 84113, USA
[5]Department of Pediatrics, University of Utah School of Medicine, Salt Lake City, UT 84112, USA
[6]Division of Hematology-Oncology, Arthur and Sonia Labatt Brain Tumour Research Centre, Department of Pediatrics, Hospital for Sick Children, University of Toronto, Toronto, ON M4N1X8, Canada
[7]Lead Contact
*Correspondence: rodney.stewart@hci.utah.edu
http://dx.doi.org/10.1016/j.celrep.2016.09.081

SUMMARY

Malignant brain tumors are the leading cause of cancer-related deaths in children. Primitive neuroectodermal tumors of the CNS (CNS-PNETs) are particularly aggressive embryonal tumors of unknown cellular origin. Recent genomic studies have classified CNS-PNETs into molecularly distinct subgroups that promise to improve diagnosis and treatment; however, the lack of cell- or animal-based models for these subgroups prevents testing of rationally designed therapies. Here, we show that a subset of CNS-PNETs co-express oligoneural precursor cell (OPC) markers *OLIG2* and *SOX10* with coincident activation of the RAS/MAPK (mitogen-activated protein kinase) pathway. Modeling NRAS activation in embryonic OPCs generated malignant brain tumors in zebrafish that closely mimic the human oligoneural/NB-*FOXR2* CNS-PNET subgroup by histology and comparative oncogenomics. The zebrafish CNS-PNET model was used to show that MEK inhibitors selectively eliminate Olig2$^+$/Sox10$^+$ CNS-PNET tumors in vivo without impacting normal brain development. Thus, MEK inhibitors represent a promising rationally designed therapy for children afflicted with oligoneural/NB-*FOXR2* CNS-PNETs.

INTRODUCTION

Pediatric tumors of the CNS are the leading cause of cancer-related deaths in children under 14 years of age. The most common pediatric brain tumors can be broadly defined as glial-like (such as astrocytoma) or embryonal-like (such as medulloblastoma [MB]) and are thought to arise from glial or multi-potent progenitors, respectively. Primitive neuroectodermal tumors of the CNS (CNS-PNETs) are embryonal tumors that comprise a complex group of highly malignant pediatric brain tumors with similar histology but diverse clinical behaviors (Adamski et al., 2014; Chan et al., 2015). Histologically, CNS-PNETs closely resemble cerebellar MB, but only comprise ~10% of MB cases, and are often localized in the cerebral hemispheres (Chan et al., 2015). The lack of robust diagnostic markers combined with the rare occurrence of CNS-PNETs often leads to misdiagnosis and treatment with heterogeneous regimens, which likely contributes to the dismal overall survival of CNS-PNET patients despite aggressive treatments that include surgery, radiation, and chemotherapy. Indeed, CNS-PNET patients have a 5-year overall survival rate of 20%–40%, in contrast to 60%–65% observed in high-risk metastatic MB (Chan et al., 2015). Clearly, new treatments are needed to improve survival and morbidity in children with CNS-PNETs.

Recent comparative genomic analysis has classified CNS-PNETs into distinct subgroups with unique molecular signatures and/or genetic aberrations (Picard et al., 2012; Sturm et al., 2016). These studies promise to improve diagnosis and guide the use of more selective, subgroup-specific therapies that both increase patient survival and alleviate long-term cognitive and physical side effects. However, a current barrier to identifying such treatments is the lack of cell- or animal-based models of CNS-PNET subgroups to test potential therapies, which is likely due to both the rarity of these tumors and the lack of defined cellular origins and oncogenic drivers for each subgroup. Here, we present a genetically engineered animal model of the CNS-PNET subgroup that is defined by the expression of oligoneural precursor cell (OPC) genes, such as *OLIG2* and *SOX10*, previously referred to as oligoneural PNET (Picard et al., 2012) or CNS_NB-*FOXR2* (Sturm et al., 2016). We show that *SOX10*-expressing OPCs represent an origin of the oligoneural CNS-PNET subgroup by activating NRAS/MAPK (mitogen-activated protein kinase) signaling in these cells. The zebrafish CNS-PNET-like tumors show conservation of histopathology (small round neuroblastic cells of primitive neuroectodermal origin) and hallmarks of the oligoneural CNS-PNET subtype, including

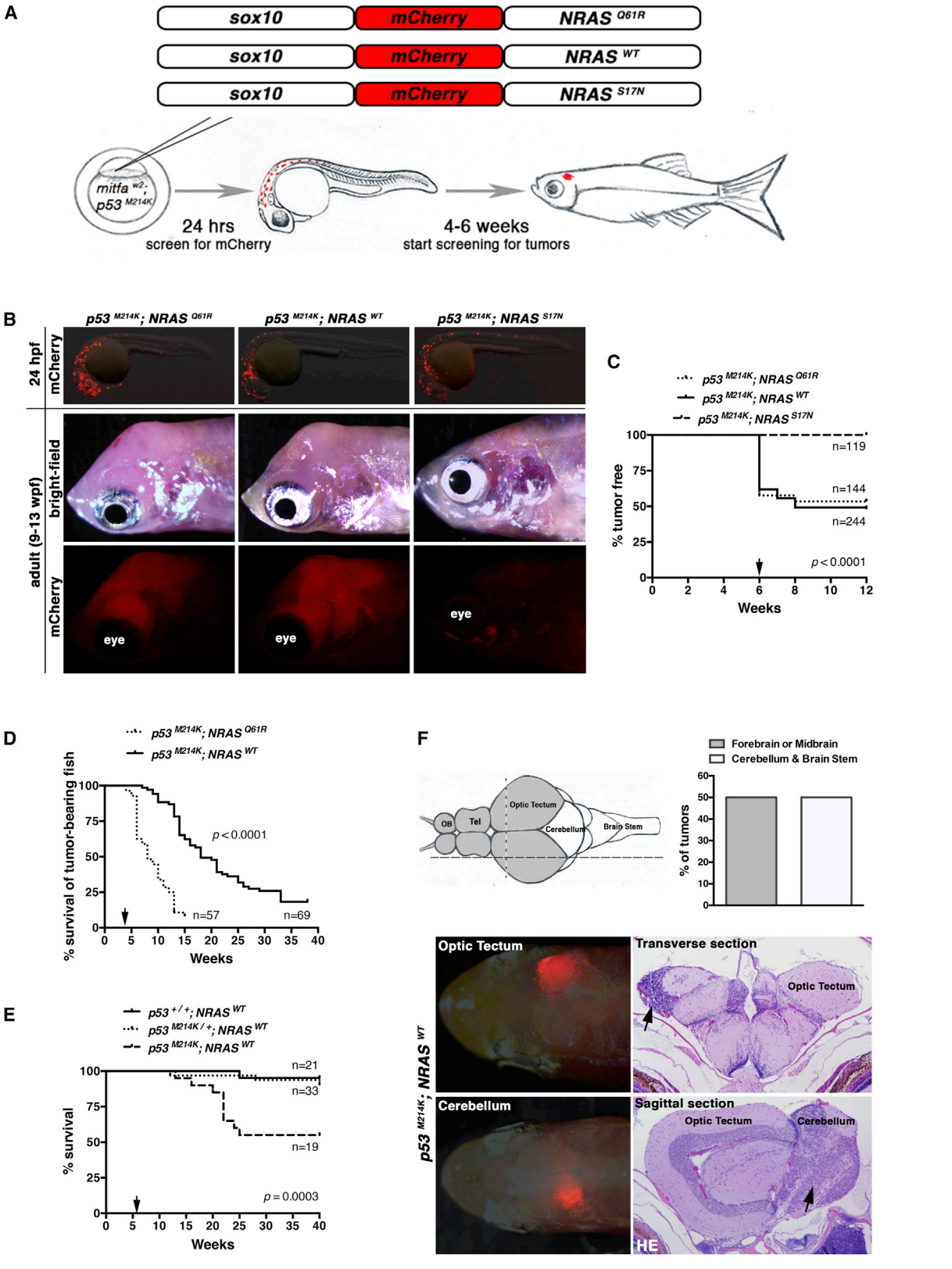

(legend on next page)

Sox10 and Olig2 co-expression. Comparative genomic analysis also revealed remarkable conservation between the molecular signaling pathways and differentiation states of zebrafish and human oligoneural/NB-*FOXR2* CNS-PNETs. Finally, we describe a drug-screening platform using orthotopic embryonic brain tumor transplantation in immune-competent animals to rapidly screen drugs that eliminate these highly aggressive tumors without affecting the development of the rest of the animal and identify MEK inhibitors as a promising therapeutic option for selectively eliminating *OLIG2*/*SOX10*-expressing CNS-PNETs in children. Thus, the zebrafish brain tumor modeling and drug treatment approaches outlined here, combined with its well-established embryology and imaging properties, provide a powerful and rapid in vivo method of identifying conserved developmental, cellular, and molecular mechanisms in childhood brain cancers, as well as accelerating subgroup-specific drug discovery through whole-animal-based, small-molecule screening.

RESULTS AND DISCUSSION

A Subset of Human CNS-PNETs Express OPC Markers Coincident with Activation of MAPK Signaling

Recent studies identified a subset of CNS-PNETs with elevated expression of *OLIG2* and *SOX10* mRNA (Picard et al., 2012; Sturm et al., 2016), a combination typically restricted to embryonic OPCs and oligodendrocytes during brain and CNS development (Weider and Wegner, 2016). Consistent with these findings, analysis of CNS-PNET gene expression datasets (Li et al., 2009) showed that 8/26 CNS-PNETs co-expressed elevated levels of *SOX10* and *OLIG2* mRNA (Figure S1A), a significant correlation ($p < 0.0001$) for this class of pediatric brain tumors (Figure S1B). Analysis of an MB gene expression dataset (Kool et al., 2008) also showed that a small fraction of MBs co-expressed *OLIG2* and *SOX10* mRNA (Figure S1C); however, this correlation was not significant (Figure S1B). To determine whether OLIG2 and SOX10 proteins are co-expressed in CNS-PNETs and MB, we performed immunohistochemical (IHC) analysis on four CNS-PNETs and 52 MB patient samples, which showed co-expression in one of four CNS-PNETs and 1 of 52 MB samples (Figure S1D). Together, these findings show that approximately 25%–30% of embryonal CNS-PNET tumors, and some rare MBs, co-express SOX10 and OLIG2 in cells that maintain the histological morphology of undifferentiated glial progenitors such as OPCs.

CNS-PNETs that co-express *OLIG2* and *SOX10* have significantly elevated *ERBB3* mRNA levels (Figures S1A and S1E). As ERBB3 is an upstream activator of RAS GTPases (Hynes and MacDonald, 2009), we next determined whether the RAS/MAPK signaling pathway was activated in *OLIG2*$^{+}$/*SOX10*$^{+}$ double-positive tumors. Gene set enrichment analysis (GSEA) of *OLIG2*/*SOX10*-expressing CNS-PNET tumors compared to all other CNS-PNETs revealed a significantly enriched RAS pathway signature (Figure S1F). Consistent with these findings, phosphorylated MAPK (pMAPK) levels were elevated in human CNS-PNET and MB tumor samples co-expressing OLIG2 and SOX10 (Figure S1D). Elevated pMAPK staining was also observed in two additional CNS-PNETs and nine MBs (as represented in Figure S1D). These studies suggest that a subset of human CNS-PNETs and MBs may be driven by activation of the MAPK pathway, a finding consistent with previous studies showing RAS/MAPK pathway activation in MB (Gilbertson et al., 2006; MacDonald et al., 2001).

Oncogenic and Wild-Type NRAS Expression in OPCs Induces CNS Tumors in Zebrafish

To functionally test whether CNS-PNETs could originate from OPCs with RAS/MAPK activation, we generated DNA constructs that drive human *NRAS* expression in embryonic OPCs using an established *sox10* promoter (Kirby et al., 2006). *NRAS* was either oncogenic with a GTPase-activating mutation [*Tg(sox10:mCherry-NRAS*^{Q61R}*)*], wild-type (WT) [*Tg(sox10:mCherry-NRAS*^{WT}*)*], or disabled with a GTPase-inactivating mutation [*Tg(sox10:mCherry-NRAS*^{S17N}] (Figures 1A and 1B). Up to 88% of CNS-PNETs have *p53* pathway dysfunction in sporadic tumors (Eberhart et al., 2005), and Li-Fraumeni syndrome patients are predisposed to CNS-PNET formation (Orellana et al., 1998). As such, the *NRAS* DNA constructs were injected into embryos homozygous for the *p53*^{M214K} loss-of-function mutation (Berghmans et al., 2005) to generate potentially tumor-bearing animals containing a randomly integrated (chimeric) *NRAS* transgene (Figures 1A and 1B). To aid tumor visualization, all animals

Figure 1. Oncogenic and WT NRAS Drive CNS Tumors in Zebrafish

(A) Schematic of DNA constructs injected into one-cell-stage *mitfa*^{w2}*; p53*^{M214K} embryos and timeline for injections and screening of tumors arising from mosaic expression of the *sox10:mCherry-NRAS* constructs in (B)–(F).

(B) Top panels show detection of chimeric expression of *sox10:mCherry-NRAS* constructs by immunofluorescence in lateral views of 24-hpf embryos to confirm injection efficiency. Only embryos that expressed mCherry at 24 hpf were raised for tumor and survival analysis in (C)–(E), but not all mCherry-expressing 24-hpf embryos would eventually develop tumors. Middle (bright-field) and bottom (mCherry) panels show a tumor mass arising in the head in *NRAS*^{Q61R}- and *NRAS*^{WT}-expressing fish but not *NRAS*^{S17N}-expressing fish.

(C) Percentage of *mitfa*^{w2}*; p53*^{M214K} embryos injected with one of the indicated constructs that went on to develop tumors after 6 weeks (arrow).

(D) Survival of tumor-bearing *mitfa*^{w2}*; p53*^{M214K} animals injected with indicated constructs analyzed after 4 weeks post-injection (arrow).

(E) p53 dependence of *NRAS*^{WT}-driven tumors. The *Tg(sox10:mCherry-NRAS*^{WT}*)* construct was injected into embryos derived from an incross between *mitfa*^{w2}*; p53*$^{M214K/+}$ fish and analyzed for survival. Representative results from three independent injections are shown in (C)–(E).

(F) Top left: schematic of zebrafish brain with forebrain and midbrain regions shaded gray, while cerebellum and brain stem are white. Olfactory bulb (OB) and telencephalon (Tel) are indicated. Vertical (stippled) and horizontal (dashed) lines indicate the locations of transverse and sagittal histological sections in histology at the bottom right. Top right: *NRAS*^{WT}-driven brain tumors arise equally in the indicated compartments of the zebrafish brain. Averages correspond to two independent experiments, both of which gave rise to values of 50%. Forebrain or midbrain (gray bar) is indicated by gray shading, and cerebellum or brain stem (white bar) is indicated by white shading in schematic. Bottom: tumors arising in the optic tectum or cerebellum were detected by directly visualizing mCherry and confirmed by histology on indicated sections (black arrows show location of tumors).

See also Figure S1.

were also homozygous for the *mitfa*^{w2} mutation that eliminates pigment (melanophore) formation (Lister et al., 1999). By 6 weeks post-fertilization (wpf), *mitfa*^{w2}; *p53*^{M214K}; *Tg(sox10:mCherry-NRAS*^{Q61R}*)* embryos displayed CNS tumors at a frequency of ~50% (Figure 1C). Surprisingly, we observed CNS tumors at a similar penetrance in *mitfa*^{w2}; *p53*^{M214K}; *Tg(sox10:mCherry-NRAS*^{WT}*)* zebrafish (Figure 1C), although tumors induced by activated *NRAS*^{Q61R} were more aggressive and showed poorer overall survival (Figure 1D). Importantly, the expression of GTPase-disabled NRAS [*mitfa*^{w2}; *p53*^{M214K}; *Tg(sox10:mCherry-NRAS*^{S17N}*)*] did not give rise to tumors (Figure 1C), indicating that activation of downstream NRAS effectors is still required for *mitfa*^{w2}; *p53*^{M214K}; *Tg(sox10:mCherry-NRAS*^{WT}*)*-induced oncogenesis. Loss of p53 function was also a critical component (Figure 1E). These data suggest that uncontrolled expression of WT NRAS in embryonic neural stem cell populations may be sufficient to drive tumorigenesis in a subset of human pediatric brain tumors. Consistent with this notion, examination of *NRAS* mRNA levels in published human tumor databases (https://www.oncomine.org) showed that *NRAS* mRNA is highly expressed in a number of embryonal brain tumors when compared to normal brain: MB (36- to 50-fold), CNS PNET (51-fold), and atypical teratoid/rhabdoid tumors (AT/RTs, 250-fold) (Pomeroy et al., 2002). Thus, our finding that elevated WT NRAS, together with p53 deficiency, is sufficient for CNS-PNET tumorigenesis may provide at least one possible explanation for why mutations in RAS/MAPK pathway components are rarely observed in pediatric brain tumors, despite reports that these tumors exhibit robust RAS/MAPK pathway activation (Gilbertson et al., 2006; Sturm et al., 2016). Future sequencing analysis in CNS-PNET patient samples may identify additional mechanisms for RAS/MAPK activation in CNS-PNETs (e.g., NF1 loss, SOS gain) and determine whether mutations in additional p53 pathway components are associated with RAS/MAPK activation, as predicted by this model.

Zebrafish Brain Tumor Histology and Location Are Consistent with Human CNS-PNETs

Pediatric CNS-PNET tumors are primarily diagnosed based on location, H&E-based cell morphology, and specific IHC markers (Chan et al., 2015; Louis et al., 2007). Tumors that are composed of small blue cells and localized in the cerebrum, brain stem, or spinal cord are likely to be diagnosed as CNS-PNETs, or as AT/RTs if they lack *INI1/SNF5* staining, whereas those localized in the cerebellum would be primarily diagnosed as MBs (Chan et al., 2015). Therefore, to determine the extent to which the NRAS-driven zebrafish brain tumors resemble human pediatric tumors, we first analyzed zebrafish tumor location and histology. We focused our analysis on the *mitfa*^{w2}; *p53*^{M214K}; *Tg(sox10:mCherry-NRAS*^{WT}*)* tumors generated by transient DNA injections (outlined in Figure 1A and hereinafter referred to as *NRAS*^{WT}-driven tumors) due to the previously reported finding that *NRAS* expression is elevated in embryonal brain tumors (Pomeroy et al., 2002), whereas *NRAS* mutational activation is less common (Gilbertson et al., 2006). We found that *NRAS*^{WT}-driven tumors arise both in the anterior lobes (primarily the optic tectum) and in the hindbrain, including the cerebellum and brain stem (Figure 1F). Thus, the zebrafish tumors arise in locations consistent with embryonic brain tumors such as CNS-PNETs (cerebrum and brain stem) and MBs (cerebellum).

As the majority of human CNS-PNETs are located in the cerebrum, we next performed histological analysis on three zebrafish tumors arising in the anterior compartments (Figure 2A). H&E staining showed tightly packed and undifferentiated small, round blue cells with a high nuclear-to-cytoplasmic ratio, reminiscent of human CNS-PNETs (Figure 2A). IHC analysis confirmed the expression of markers commonly used to diagnose human CNS-PNETs, including nestin, synaptophysin, and focal Gfap (glial fibrillary acidic protein) staining (Figure 2A). Tumors also stained positive for Ini1 (Snf5/Smarcb1), which excluded the possibility that they are AT/RTs (Figure 2A) (Chan et al., 2015). Thus, based on histology, the *NRAS*^{WT}-driven tumors arising from the anterior compartments most closely resemble human CNS-PNETs.

To determine whether the *NRAS*^{WT}-driven CNS-PNET-like tumors display OPC characteristics, we analyzed Olig2 and Sox10 expression and detected strong positive staining (Figure 2A). The tumors also expressed NRAS (derived from the transgene) and pMAPK (Figure 2A). To complement our IHC analyses, we also performed live confocal imaging in zebrafish fluorescent reporter lines to visualize *olig2*-positive (GFP+) cells and *sox10*-driven mCherry-NRAS within developing tumors (Figure 2B). This analysis showed that mCherry-NRAS^{WT} and GFP were co-expressed in tumor cells with a rounded cellular morphology consistent with the primitive neuroblastic appearance detected by histology, while in adjacent normal brain tissue, GFP was expressed in oligodendrocytes with typical elongated and dendritic morphology (Figure 2B).

Genomic Analysis Shows Zebrafish Brain Tumors Genetically Resemble Human CNS-PNETs

To determine whether the zebrafish CNS-PNET-like tumors resemble human CNS-PNET tumors at the genetic level, we compared gene expression signatures between zebrafish *NRAS*^{WT}-driven tumors and human CNS-PNETs. We first performed RNA sequencing (RNA-seq) analysis on *NRAS*^{WT}-expressing zebrafish brain tumors derived from the anterior compartments, as well as normal brain tissue, and identified differentially expressed gene signatures indicative of signaling pathway activation by GSEA (Figure 3A). The analysis was predictive of an embryonic progenitor origin, with significant enrichment for genes expressed in pediatric tumors, embryonic stem (ES) cells, and the epithelial-to-mesenchymal transition (EMT), while gene sets for differentiated neurons and synaptic transmission were negatively enriched (Figure 3A, see the neuronal gene set). Oncogenic signatures revealed enrichment for genes regulated by the epidermal growth factor (EGFR) pathway (Figure 3A), which is consistent with the prevalence of pMAPK in the human CNS-PNETs (Figure S1D). In addition, the zebrafish tumors likely have a dysfunctional retinoblastoma (Rb) 1 (Rb1) pathway, since gene sets predictive of Rb1 loss and E2F transcription factor activation were significantly enriched (Figure 3A), consistent with the occurrence of CNS-PNETs in some Rb patients (Li et al., 2005) and loss of Rb causing embryonal-like brain tumors in mouse and zebrafish (Jacques et al., 2010; Saab et al., 2009; Solin et al., 2015).

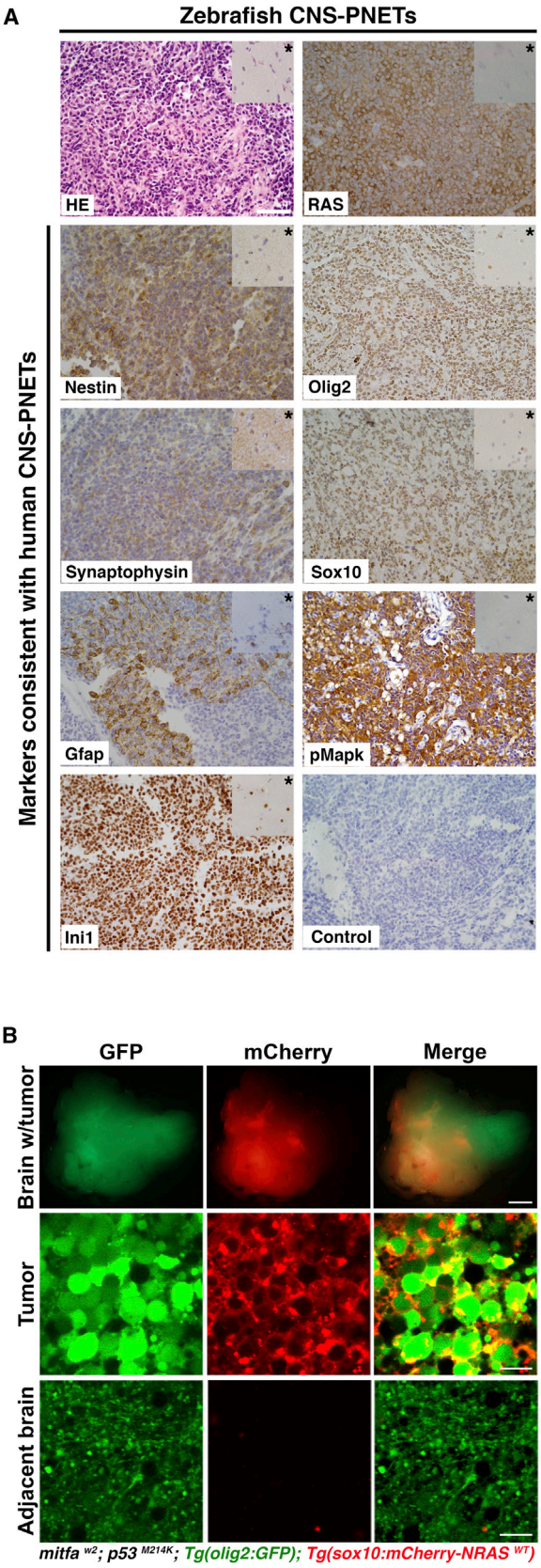

Figure 2. Zebrafish *NRAS*^{WT}-Driven Brain Tumors Derived from the Anterior Brain Closely Resemble Oligoneural CNS-PNET Tumors

(A) Shown is a representative example of the histology (H&E [HE]) and IHC analysis (indicated in each panel) from three independent zebrafish brain tumors arising in the anterior lobes of *NRAS*^{WT}-expressing fish. Inset in each top right corner (indicated by a star) shows staining in the adjacent normal brain area. Scale bars, 50 μm.

(B) Top panels show a confocal image of a live stable transgenic [*mitfa*^{w2}; *p53*^{M214K}; *Tg(olig2:GFP)*] zebrafish brain with an optic tectum tumor expressing *Tg(sox10:mCherry-NRAS*^{WT}*)*. Middle panels show that the tumor is composed of large undifferentiated cells expressing GFP in the cytoplasm and mCherry at the membrane. Bottom panels show typical elongated oligodendrocytes in the adjacent tumor-free area. Scale bars, 500 μm (brain with tumor) and 10 μm (tumor and adjacent brain).

Human CNS-PNETs have recently been stratified based on gene expression analysis, with high levels of both *OLIG2* and *SOX10* associated with the oligoneural (Picard et al., 2012) or CNS_NB-*FOXR2* (Sturm et al., 2016) subgroups (Figure S2A). To determine whether the zebrafish CNS-PNET-like tumors resemble these specific subtypes, we performed comparative genomic analysis between human and zebrafish tumors (Figure 3B; Table S1). We first identified the top 60 up- or downregulated genes in *OLIG2*/*SOX10* co-expressing human tumors compared to normal human brain (Li et al., 2009) and compared this list to the differentially expressed genes in zebrafish CNS-PNET-like tumors compared to normal zebrafish brain (see Experimental Procedures). This analysis showed that zebrafish CNS-PNET-like tumors share a highly conserved gene expression signature with the human oligoneural CNS-PNET subtype (Figure 3B). Furthermore, when we compared the zebrafish CNS-PNET-like tumors to all human CNS-PNET brain tumor subgroups using principal-component analysis (PCA) with published gene lists (Picard et al., 2012; Sturm et al., 2016), we found that the zebrafish tumors are most similar to the oligoneural and NB-*FOXR2* CNS-PNET subgroups (Figure 3C). We also found that the zebrafish CNS-PNET-like tumors are more similar to human oligoneural/NB-*FOXR2* CNS-PNETs than zebrafish normal brain (Figure 3C). Consistent with the PCA findings, analysis of the recently described CNS_NB-*FOXR2* subgroup (Sturm et al., 2016) showed that these tumors also have significant correlation with elevated expression of *SOX10*/*OLIG2* ($p < 0.0001$) and ERBB3 ($p < 0.0001$) and positively enriched for RAS/MAPK pathway activation by GSEA (Figures S2B–S2D). These data suggest that the oligoneural CNS-PNET (Picard et al., 2012) and CNS_NB-*FOXR2* (Sturm et al., 2016) subgroups represent a single tumor entity in humans that can be distinguished from other CNS-PNET subgroups by high *SOX10*/*OLIG2* co-expression. Importantly, these analyses indicate that zebrafish CNS-PNET-like brain tumors represent an animal model for the oligoneural/NB-*FOXR2* CNS-PNET subgroup.

Orthotopic Tumor Transplantation Assay Identifies MEK Inhibitors as Potential Therapies for OLIG2/SOX10-Expressing CNS-PNETs

There are no established cell lines or animal models of the oligoneural/NB-*FOXR2* CNS-PNET subtype, which limits our ability to discover new therapies that specifically target these tumors. Therefore, we used the zebrafish oligoneural CNS-PNET model

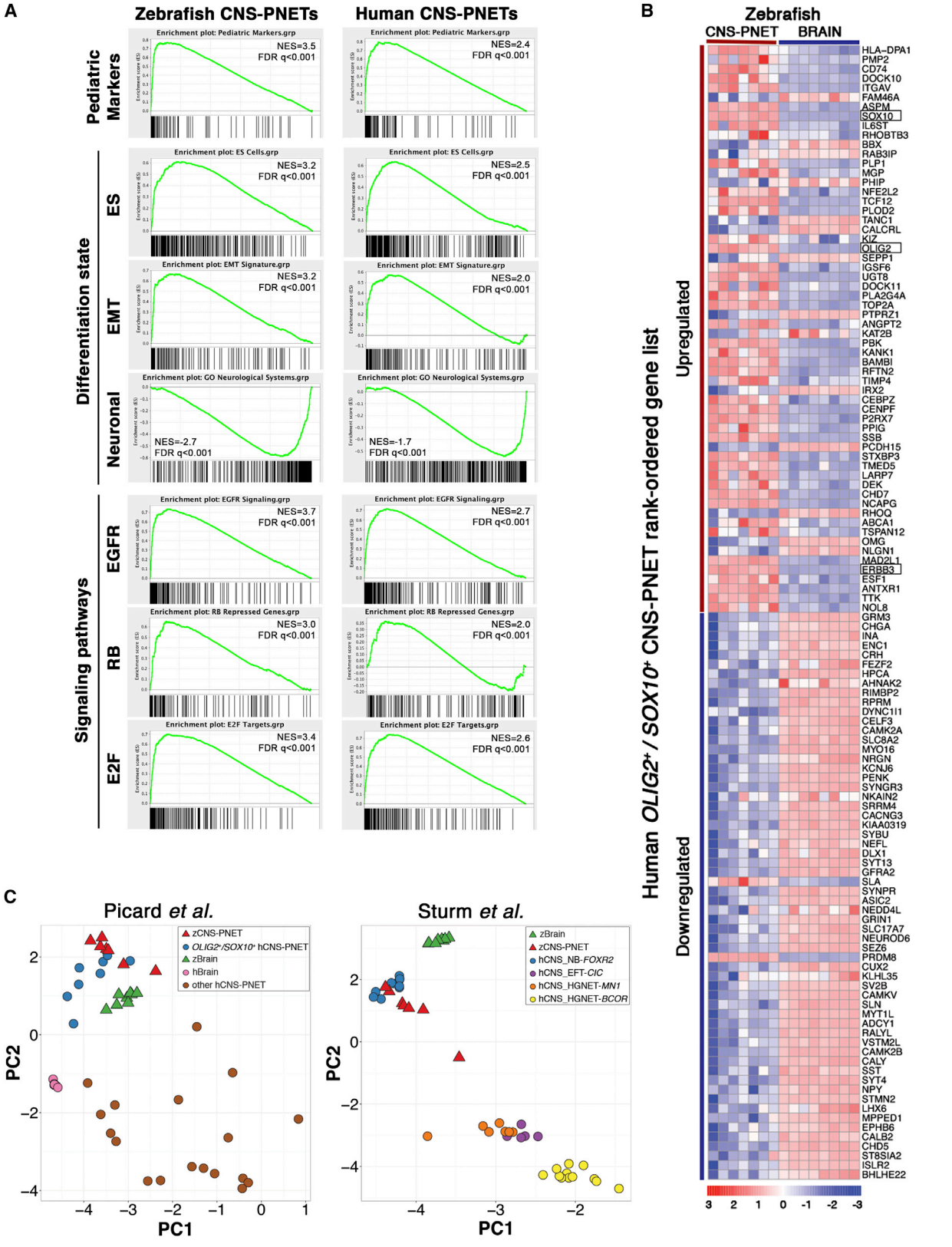

(legend on next page)

to identify potential therapies for OLIG2/SOX10-expressing CNS-PNET tumors. We first developed an orthotopic tumor cell transplantation method using embryonic zebrafish at 2 days post-fertilization (dpf) that allows the rapid propagation and direct visualization of primary brain tumor cells into hundreds of embryos per day with 80%–90% engraftment efficiency, as the adaptive immune system has yet to mature at this stage (Figure 4A). Single-cell suspensions derived from *NRAS*^{WT}-driven CNS-PNETs were delivered to the lumen of the fourth ventricle (Figure 4A). At 1 day post-transplantation, the tumor cells could be visualized by fluorescence microscopy within the developing brain tissue and cerebral spinal fluid (Figure 4A, 3 dpf, arrows). Transplanted tumors spread throughout the brain by 17 dpf and encompassed the entire brain by 7 wpf (Figure 4A).

Next, we developed a drug treatment regimen (Figure 4B) to test whether inhibition of the Mapk pathway could prevent tumor growth in vivo. The AZD6244 compound (ARRY-142886) is an established MEK inhibitor that is under clinical investigation for the treatment of multiple cancers, including childhood brain tumors (ClinicalTrials.gov: NCT01386450). A representative group of embryos were imaged prior to treatment (Figure 4C, 3 dpf). Embryos were then randomly divided into groups, treatments were initiated, and embryos were monitored daily for a 5-day period. Upon completion of treatments (8 dpf), embryos were imaged by fluorescence microscopy, and tumor area was quantified (Figure 4C). AZD6244-treated embryos exhibited a significantly smaller tumor burden post-treatment compared to DMSO-treated embryos (Figure 4C). Similar results were obtained with the MEK inhibitor U0126 (Figures S3A and S3B). DMSO- and inhibitor-treated embryos had similarly high survival rates during the course of the 5-day treatment (Figure 4D; Figure S3C). In addition, immunoblot staining from tumor lysates showed that MAPK phosphorylation was significantly diminished in the MEK-inhibitor-treated tumors (Figure 4E). To determine whether the AZD6244 treatment translated into a durable response, we next monitored the juvenile and adult fish from both AZD6244 and DMSO treatment groups weekly for 8 weeks. Remarkably, only 21% of the AZD6244-treated fish displayed visible tumors at 8 weeks post-treatment compared to 88% of the DMSO-treated fish (Figure 4F; Movies S1 and S2), and AZD6244-treated fish exhibited a significantly higher post-treatment survival (Figure 4D). In addition, many of the DMSO-treated tumors had metastasized throughout the spinal cord by 8 weeks post-treatment, while none of the AZD6244-treated tumor fish showed evidence of metastasis (Movies S1 and S2). These results show that MEK inhibitors are extremely effective at eliminating *sox10/olig2*-expressing CNS-PNET in vivo and, at the doses and times used, confer minimal toxicity to WT tissues.

In summary, we show that activation of NRAS signaling in *sox10*-expressing zebrafish OPCs drives the formation of CNS PNET-like tumors that share remarkable conservation with human oligoneural/NB-*FOXR2* CNS-PNETs. We take advantage of the scalability and imaging properties of the zebrafish system to design a rapid drug-screening platform and show that MEK inhibitors potently and durably reverse CNS-PNET-like growth in vivo without obvious effects on other tissues, including the developing brain. Thus, our findings suggest that MEK inhibitors could be an effective therapeutic approach for children with embryonal tumors expressing *SOX10* and *OLIG2*. Furthermore, these studies provide the foundation to rapidly evaluate potential genetic drivers of different CNS tumors in zebrafish, including candidate fusion oncogenes and epigenetic modifiers identified in large-scale genomic screens for MB and pediatric glioma (Pashos et al., 2013). Our phenotypic drug-screening platform also provides a complementary approach to allow rapid and inexpensive identification of compounds that reverse tumor growth, invasion and/or metastasis of brain cancers. Finally, the embryonic brain transplantation method could be readily modified to accommodate human cancer cells to generate patient-derived xenograph (PDX) models of childhood brain cancers for future small-molecule drug screening, similar to methods described for adult glioblastoma cell lines (Welker et al., 2016).

EXPERIMENTAL PROCEDURES

Zebrafish Lines

Zebrafish were maintained and bred as described previously (Westerfield, 1993), and all procedures were approved by the University of Utah Institutional Animal Care and Use Committee.

Tumor Generation, Tumor Onset, and Survival

At 24 hr post-injection of DNA constructs, embryos were screened and sorted for the expression of mCherry. Starting at 4–6 weeks, fish were screened weekly using a wide-fluorescence microscope for the onset of red tumor masses in the CNS. To generate survival curves, *mitfa*^{w2}; *p53*^{M214K} tumor-bearing fish injected with *sox10:mCherry-NRAS*^{WT} (two sets, n = 69) or *sox10:mCherry-NRAS*^{Q61R} (three sets, n = 57) were monitored visually in tanks weekly and by fluorescence microscopy bi-weekly. Fish were sacrificed when tumor burden increased to approximately 20% of the total body size or impaired the animal's ability to swim, feed, or behave normally. Thus, values plotted in the survival curve (Figure 1D) are determined by the date of sacrifice. For details about the injection procedure, preservation of culled fish, and experiments using *mitfa*^{w2}; *p53*^{M214K} fish, see Supplemental Experimental Procedures.

Figure 3. Zebrafish *NRAS*^{WT}-Driven Tumors Show Gene Expression Signatures that Are Predictive of Oligoneural Progenitors and Pediatric Tumors

(A) Gene set enrichment analysis (GSEA) was performed on genes that were differentially expressed between *NRAS*^{WT}-driven tumors and normal zebrafish brain (left) or genes that were differentially expressed between published human CNS-PNETs (GEO: GSE14295) and normal fetal brain (right). Gene sets identified in these analyses and their general biological categories are indicated to the left. NES, normalized enrichment score; FDR, false discovery rate; ES, embryonic stem; EMT, epithelial-mesenchymal transition.

(B) Heatmap showing gene expression in zebrafish *NRAS*^{WT}-derived tumors and normal brain tissue arranged to highlight comparison to the top 60 genes up- and downregulated in human *OLIG2*$^{+}$/*SOX10*$^{+}$ CNS-PNETs compared to fetal brain. *SOX10*, *OLIG2*, and *ERBB3* genes are highlighted.

(C) Principal-component analysis (PCA) showing zebrafish *NRAS*^{WT}-derived tumors cluster with the *OLIG2*/*SOX10*-expressing human CNS-PNETs based on the oligoneural gene list generated by Picard et al. (2012) or the CNS_NB-*FOXR2* gene list generated by Sturm et al. (2016). z, zebrafish; h, human.

See also Figure S2 and Tables S1 and S2.

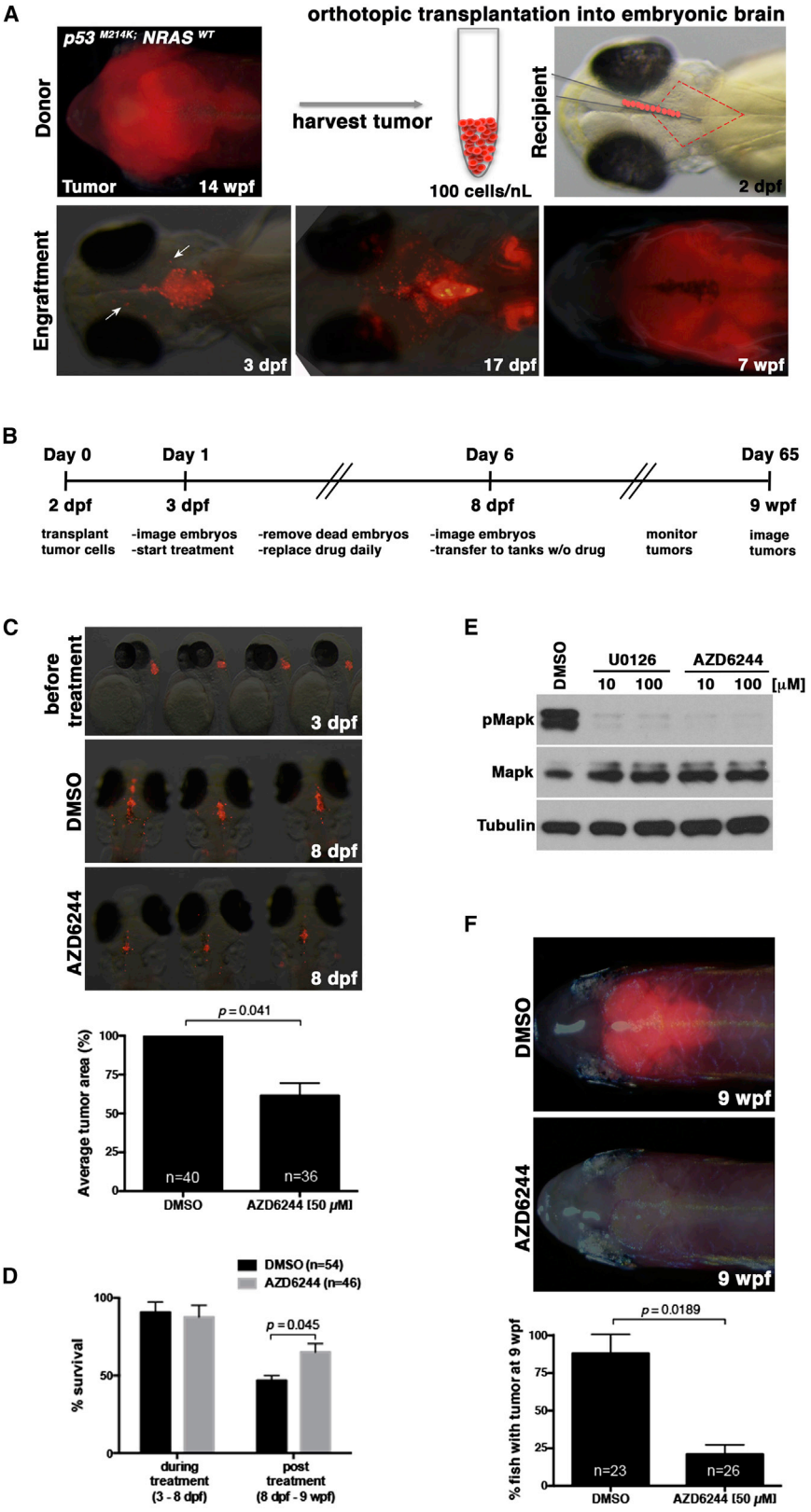

Figure 4. Drug Screens Using an Embryonic Brain Tumor Transplantation Assay Identify MEK as a Therapeutic Target for Oligoneural/*NB-FOXR2* CNS-PNET-like Tumors

(A) Tumors derived from the anterior brain of *mitfa*^{w2}; *p53*^{M214K}; *Tg(sox10:mCherry-NRAS*^{WT}) transgenic fish were harvested and injected into the fourth ventricle (outlined in red) of a 2-dpf *mitf*^{w2} embryo (top panels). The following day (3 dpf), successful injections were visualized by immunofluorescence, and some tumor cells could be found in the surrounding brain (arrows). By 17 dpf, tumor cells had proliferated and invaded the surrounding tissue. At 7 wpf, the tumor cells had spread throughout the brain.

(B) Schematic describing the timeline for the orthotopic embryonic transplantation method and drug treatment.

(C) Representative images of mCherry expression in embryos at 24 hr post-transplantation before treatment (3 dpf) and embryos treated daily for 5 days (8 dpf) with DMSO or MEK inhibitor AZD6244. Quantification of immunofluorescence on the final day of treatment (8 dpf) shows a significant decrease in the transplanted tumor mass in AZD6244-treated embryos compared to control.

(D) Survival analysis of embryos during drug treatment (3–8 dpf) shows that DMSO and AZD6244 do not cause significant toxicity at doses used, while survival analysis from 8 dpf to 9 wpf shows that AZD6244-treated embryos have significantly higher post-treatment survival ($p = 0.045$). Averages in (C) and (D) represent three independent experiments (±SEM) for each panel.

(E) Western blot showing that MEK inhibitors U0126 and AZD6244 inhibit Mapk signaling in zebrafish *NRAS*^{WT}-driven brain tumor cells treated ex vivo. (For U0126 treatment results, see Figure S3).

(F) Representative images of the majority of 9-wpf adult fish at 8 weeks post-treatment (top) and quantification (bottom) from three independent experiments. Error bars represent ±SEM.

See also Figure S3 and Movies S1 and S2.

Orthotopic Embryonic Transplants

Tumor cells were injected into the fourth ventricle of each embryo and then transferred into fresh egg water. Twenty-four hours later, embryos were screened using a fluorescent microscope to ensure consistent engraftment sizes. Successfully transplanted embryos were placed in tanks to grow or treated with drugs, as described later. For further details about the transplantation procedure, see Supplemental Experimental Procedures.

In Vivo Drug Treatment

Transplants were randomly distributed into two treatment groups: DMSO or drug (AZD6244 or U0126). Embryos were placed in 12-well plates, 10–12 per well in 0.5 mL of egg water with either DMSO or 50 μM drug, and plates were moved to 28°C. Treatments were refreshed daily for 5 days. Embryos were imaged and rinsed with egg water, and each treatment group was combined and placed in separate tanks to grow for 8 weeks. At 9 wpf, fish were screened by fluorescence microscopy for presence of a tumor mass and euthanized with Tricaine-S. For further details about both in vivo and ex vivo drug treatment, see Supplemental Experimental Procedures.

Transplant Quantification

Fluorescent images of tumor transplants were acquired on the fifth day of treatment (8 dpf). Tumor area for each embryo was quantified using ImageJ. For each treatment, the average tumor area was calculated after removing the smallest and largest numbers (to control for outliers). Average tumor area for DMSO-treated embryos was set to 100% for each experiment. Detailed quantification procedures are described in Supplemental Experimental Procedures.

GSEA, Heatmaps, and PCA

Rank lists for GSEA were generated using zebrafish normal brain (n = 8) versus tumor (n = 7) and human normal brain versus CNS-PNETs (GEO: GSE14295; 26 CNS_PNETs and 7 normal fetal brains). Analysis was performed using GSEA v2.2.2 (http://www.broadinstitute.org/gsea).

The human CNS-PNET rank-ordered gene list was generated from the GEO: GSE14295 dataset (eight OLIG2/SOX10 high CNS PNETs and seven normal fetal brains). To generate heatmaps, human genes were ranked based on fold change. Human genes that were not present in the zebrafish dataset (i.e., human ortholog not present in zebrafish) were removed. The top 60 up- and downregulated genes were then selected for comparison to zebrafish tumors (RNA-seq datasets from zebrafish tumors and control brains can be accessed via GEO: GSE80768). Zebrafish tumor and normal brain gene expression with $p < 0.05$ was represented using mean centered $\log_2$ FPKM (fragments per kilobase of exon per million fragments mapped) values. For further details about RNA-seq analysis and the generation of heatmaps, see Supplemental Experimental Procedures.

PCA of human and zebrafish samples was performed based on published gene lists defining CNS-PNET subtypes (Picard et al., 2012; Sturm et al., 2016). Human microarray expression (GEO: GSE14295 and GSE73038) and zebrafish RNA-seq FKPM values were $\log_2$ transformed and then mean centered and scaled by sample. PCA data were generated using the R function prcomp (R 3.2.2) with centering and scaling turned off. Plots show the scores for the first two principal components.

Western Analysis, Immunohistochemistry, Cloning, and Image Acquisition and Processing

Phospho-p44/42 MAPK (Erk1/2)(Thr202/Tyr204) antibody (cat. no. 9101) from Cell Signaling Technology was used in immunohistochemistry on human and zebrafish tumor samples. For detailed procedures, see the Supplemental Experimental Procedures.

Statistical Analysis

The statistical calculations were performed using GraphPad Prism software. The Mantel-Cox test was used to calculate the statistical significance of animal survival data. The Student's t test was used to evaluate statistical significance for embryonic transplant quantification and drug treatment survival. Error bars represent ± SEM.

ACCESSION NUMBERS

The accession number for the RNA-seq data reported in this paper is GEO: GSE80768.

SUPPLEMENTAL INFORMATION

Supplemental Information includes Supplemental Experimental Procedures, three figures, two tables, and two movies and can be found with this article online at http://dx.doi.org/10.1016/j.celrep.2016.09.081.

AUTHOR CONTRIBUTIONS

K.M., E.F.B., and R.A.S. designed the study. K.M., E.F.B., R.R.M., D.A., M.K., and W.O. performed the experiments. T.J.P., J.D.S., R.J., and A.H. contributed human samples and expertise on human pediatric brain cancer. D.A. created the illustrations. K.M., E.F.B., T.L.M., D.P., C.A.J., A.H. and R.A.S. analyzed the data and prepared the manuscript, with input from all authors.

ACKNOWLEDGMENTS

We acknowledge Dr. Brian Dalley at the Huntsman Cancer Institute Core Facilities and Brett Milash at the Bioinformatics Core for assistance with RNA-seq experiments and data analysis. We thank Jim Goodman for assistance with developing the embryo transplantation assay. Samples in this study were obtained through the Primary Children's Hospital (PCH) Pediatric Cancer Program, funded by the Intermountain Healthcare Foundation and the Primary Children's Hospital Foundation, and we especially thank Melissa Cessna, Dr. Mariko Sato, Thom Jensen, and Kimberley Swaner for procurement and de-identifying patient samples. The Huntsman Cancer Institute/University of Utah provided excellent animal husbandry and maintenance. We also thank Dr. Laurence McGill at ARUP Laboratories for histology evaluations and Dr. Maura McGrail (University of Iowa) for sharing unpublished data. We are grateful to current and past members of the R.A.S. lab for discussions and critical comments on the manuscript, particularly Mattie Casey. J.D.S. is supported by an Edward B. Clark, MD Chair in Pediatric Research at the University of Utah. Funding to A.H. for this work was provided by the Canadian Institute of Health Research (CIHR; grant 137011). Funding to R.A.S. for this work was provided by the American Cancer Society (#124250- RSG-13-025-01-CSM), NIH grant (P30 CA042014 CRR program), a University of Utah Seed Grant, and the Huntsman Cancer Foundation.

Received: April 25, 2016
Revised: August 4, 2016
Accepted: September 23, 2016
Published: October 25, 2016

REFERENCES

Adamski, J., Ramaswamy, V., Huang, A., and Bouffet, E. (2014). Advances in managing medulloblastoma and intracranial primitive neuro-ectodermal tumors. F1000Prime Rep. *6*, 56.

Berghmans, S., Murphey, R.D., Wienholds, E., Neuberg, D., Kutok, J.L., Fletcher, C.D., Morris, J.P., Liu, T.X., Schulte-Merker, S., Kanki, J.P., et al. (2005). tp53 mutant zebrafish develop malignant peripheral nerve sheath tumors. Proc. Natl. Acad. Sci. USA *102*, 407–412.

Chan, T.S.Y., Wang, X., Spence, T., Taylor, M.D., and Huang, A. (2015). Embryonal Brain Tumors (New York: Springer).

Eberhart, C.G., Chaudhry, A., Daniel, R.W., Khaki, L., Shah, K.V., and Gravitt, P.E. (2005). Increased p53 immunopositivity in anaplastic medulloblastoma and supratentorial PNET is not caused by JC virus. BMC Cancer *5*, 19.

Gilbertson, R.J., Langdon, J.A., Hollander, A., Hernan, R., Hogg, T.L., Gajjar, A., Fuller, C., and Clifford, S.C. (2006). Mutational analysis of PDGFR-RAS/MAPK pathway activation in childhood medulloblastoma. Eur. J. Cancer *42*, 646–649.

Hynes, N.E., and MacDonald, G. (2009). ErbB receptors and signaling pathways in cancer. Curr. Opin. Cell Biol. *21*, 177–184.

Jacques, T.S., Swales, A., Brzozowski, M.J., Henriquez, N.V., Linehan, J.M., Mirzadeh, Z., O' Malley, C., Naumann, H., Alvarez-Buylla, A., and Brandner, S. (2010). Combinations of genetic mutations in the adult neural stem cell compartment determine brain tumour phenotypes. EMBO J. *29*, 222–235.

Kirby, B.B., Takada, N., Latimer, A.J., Shin, J., Carney, T.J., Kelsh, R.N., and Appel, B. (2006). In vivo time-lapse imaging shows dynamic oligodendrocyte progenitor behavior during zebrafish development. Nat. Neurosci. *9*, 1506–1511.

Kool, M., Koster, J., Bunt, J., Hasselt, N.E., Lakeman, A., van Sluis, P., Troost, D., Meeteren, N.S., Caron, H.N., Cloos, J., et al. (2008). Integrated genomics identifies five medulloblastoma subtypes with distinct genetic profiles, pathway signatures and clinicopathological features. PLoS ONE *3*, e3088.

Li, M.H., Bouffet, E., Hawkins, C.E., Squire, J.A., and Huang, A. (2005). Molecular genetics of supratentorial primitive neuroectodermal tumors and pineoblastoma. Neurosurg. Focus *19*, E3.

Li, M., Lee, K.F., Lu, Y., Clarke, I., Shih, D., Eberhart, C., Collins, V.P., Van Meter, T., Picard, D., Zhou, L., et al. (2009). Frequent amplification of a chr19q13.41 microRNA polycistron in aggressive primitive neuroectodermal brain tumors. Cancer Cell *16*, 533–546.

Lister, J.A., Robertson, C.P., Lepage, T., Johnson, S.L., and Raible, D.W. (1999). nacre encodes a zebrafish microphthalmia-related protein that regulates neural-crest-derived pigment cell fate. Development *126*, 3757–3767.

Louis, D.N., Ohgaki, H., Wiestler, O.D., Cavenee, W.K., Burger, P.C., Jouvet, A., Scheithauer, B.W., and Kleihues, P. (2007). The 2007 WHO classification of tumours of the central nervous system. Acta Neuropathol. *114*, 97–109.

MacDonald, T.J., Brown, K.M., LaFleur, B., Peterson, K., Lawlor, C., Chen, Y., Packer, R.J., Cogen, P., and Stephan, D.A. (2001). Expression profiling of medulloblastoma: PDGFRA and the RAS/MAPK pathway as therapeutic targets for metastatic disease. Nat. Genet. *29*, 143–152.

Orellana, C., Hernandez-Martí, M., Martínez, F., Castel, V., Millán, J.M., Alvarez-Garijo, J.A., Prieto, F., and Badía, L. (1998). Pediatric brain tumors: loss of heterozygosity at 17p and TP53 gene mutations. Cancer Genet. Cytogenet. *102*, 93–99.

Pashos, E., Park, J.T., Leach, S., and Fisher, S. (2013). Distinct enhancers of ptf1a mediate specification and expansion of ventral pancreas in zebrafish. Dev. Biol. *381*, 471–481.

Picard, D., Miller, S., Hawkins, C.E., Bouffet, E., Rogers, H.A., Chan, T.S., Kim, S.K., Ra, Y.S., Fangusaro, J., Korshunov, A., et al. (2012). Markers of survival and metastatic potential in childhood CNS primitive neuro-ectodermal brain tumours: an integrative genomic analysis. Lancet Oncol. *13*, 838–848.

Pomeroy, S.L., Tamayo, P., Gaasenbeek, M., Sturla, L.M., Angelo, M., McLaughlin, M.E., Kim, J.Y., Goumnerova, L.C., Black, P.M., Lau, C., et al. (2002). Prediction of central nervous system embryonal tumour outcome based on gene expression. Nature *415*, 436–442.

Saab, R., Rodriguez-Galindo, C., Matmati, K., Rehg, J.E., Baumer, S.H., Khoury, J.D., Billups, C., Neale, G., Helton, K.J., and Skapek, S.X. (2009). p18Ink4c and p53 Act as tumor suppressors in cyclin D1-driven primitive neuroectodermal tumor. Cancer Res. *69*, 440–448.

Solin, S.L., Shive, H.R., Woolard, K.D., Essner, J.J., and McGrail, M. (2015). Rapid tumor induction in zebrafish by TALEN-mediated somatic inactivation of the retinoblastoma1 tumor suppressor rb1. Sci. Rep. *5*, 13745.

Sturm, D., Orr, B.A., Toprak, U.H., Hovestadt, V., Jones, D.T., Capper, D., Sill, M., Buchhalter, I., Northcott, P.A., Leis, I., et al. (2016). New brain tumor entities emerge from molecular classification of CNS-PNETs. Cell *164*, 1060–1072.

Weider, M., and Wegner, M. (2016). SoxE factors: transcriptional regulators of neural differentiation and nervous system development. Semin. Cell Dev. Biol. Published online August 21, 2016. http://dx.doi.org/10.1016/j.semcdb.2016.08.013.

Welker, A.M., Jaros, B.D., Puduvalli, V.K., Imitola, J., Kaur, B., and Beattie, C.E. (2016). Standardized orthotopic xenografts in zebrafish reveal glioma cell-line-specific characteristics and tumor cell heterogeneity. Dis. Model. Mech. *9*, 199–210.

Westerfield, M. (1993). The Zebrafish Book (Eugene, OR: University of Oregon Press).